PCCP

Accepted Manuscript

ROYAL SOCIETY OF CHEMISTRY

www.rsc.org/pccp

PCCP

RSCPublishing

PAPER

In-situ Unravelling Structural Modulation across Charge-Density-Wave Transition in Vanadium Disulfide

Cite this: DOI: 10.1039/xoxxoooooox

Received ooth January 2015,
Accepted ooth January 2015

DOI: 10.1039/xoxxoooooox

www.rsc.org/

Xu Sun [a†], Tao Yao [b†], Zhenpeng Hu [c], Yuqiao Guo [a], Qinghua Liu [b], Shiqiang Wei [b*] and Changzheng Wu [a*]

Deep understanding of the relationship between electronic and structure ordering across the charge-density-wave (CDW) transition is crucial for both fundamental study and technological applications. Herein, by using in-situ x-ray absorption fine spectroscopy (XAFS) coupled with high-resolution transmission electron microscopy (HRTEM), we have illustrated the atomic-level information on the local structural evolutions across the CDW transition and its influence on the intrinsic electrical properties in VS_2 system. The structure transformation, which is featured by the formation of vanadium trimers with derivation of V–V bond length (ΔR=0.10 Å), was clearly observed across CDW process. Moreover, the corresponding influence of lattice variation on the electronic behavior was clearly characterized by experimental results as well as theoretical analysis, which demonstrated that the vanadium trimers drives the deformation of space charge density distribution into $\sqrt{3}\times\sqrt{3}$ periodicity, with the conductivity of a_{1g} band reducing by half. These observations directly unveiled the close connection between lattice evolution and electronic properties variation, paving the new avenue for understanding the intrinsic nature of electron-lattice interactions in VS_2 system and other isostructural transition metal dichalcogenides across the CDW transition process.

Introduction

Charge-density-wave (CDW) transition, which is a well-known electronic phase transition process caused by Peierls instability in low-dimensional systems, has attracted tremendous attention due to its intriguing physical mechanism and potential application in electronic devices.[1-3] During this electronic phase transition process, the charge density variation is always accompanied with periodic lattice deformation with the same wavevector.[4] Therefore, in depth analysis of the inherent connection between the modulation of lattice atom and charge density is of urgency for understanding the phase transition mechanism and expanding their applications.[5-7]

Transition metal dichalcogenides (TMDs), as a group of layered materials, have attracted great interest because of their 2D confined structure similar to graphene[8-13], as well as their potential applications in nano-electronic devices.[14,15] Meanwhile, due to the interaction between the low-dimensional structure and the electronic and phonon degrees of freedom, TMDs exhibit a wealth of electronic properties, among which the CDW behaviors is fascinating.[16-21] And tremendous efforts have been made to the research of charge density variation during the CDW process. Within the family of TMD materials, vanadium disulfide (VS_2) with triangularly packed layers of the vanadium atoms sandwiched between two layers of S atoms, is one of the most attractive CDW materials with the transition temperature near room temperature.[22,23] Previous nuclear magnetic resonance study illustrated the appearance of CDW transition in VS_2 at about 304K.[24] Angle-resolved photoemission spectroscopy, which was performed to study the electronic structure changes of VS_2 below the T_{CDW}, indicated the absence of Fermi-surface nesting in this transition process at about room temperature.[25] However, atomic-level information on the local structural evolutions, and the corresponding influence on the electrical properties during the transition process have not been revealed, hindering the understanding of underlying physical nature of electron-lattice interactions. In this regard, an accurate analysis of the structure variations in VS_2 provides an ideal approach for investigation of interplay between atomic rearrangements and electronic structure changes across CDW transition.

In this context, we analyzed the close connection between lattice variation and charge density deformation across CDW process in VS_2 system. By temperature-dependent in-situ x-ray absorption fine spectroscopy (XAFS) coupled with high-resolution transmission electron microscopy (HRTEM), the structure rearrangement with the formation of vanadium trimers in the CDW process was well characterized. Moreover, the corresponding influence of structure variation on the electronic behaviors is comprehensively discussed based on experimental results as well as theoretical analysis. These findings provide a clear model for deep analysis of the nature of electron-lattice interactions in CDW transition process.

Experimental Section

Synthesis procedure. The VS_2 sample used in this study were synthesized via the sonication reaction of $LiVS_2$ and I_2 as previously reported.[12] Firstly, the $LiVS_2$ was prepared through the reaction of V_2O_5 and Li_2CO_3 with the molar ratio of 1:1 under H_2S atmosphere at 1000 ^oC for 10h. After reaction, the black $LiVS_2$ powder was obtained. Then the as synthesized $LiVS_2$ product was mixed with the iodine powder with molar ratio $LiVS_2/I_2$ of 2:1, which was ultrasonicated in 30ml ethanol for 3h forming a black dispersion. Finally, the black product was collected by centrifugation and washed with deionized water and ethanol for several times, then dried in vacuum at 60^{o}C.

Characterization. The as-prepared samples were characterized by X-ray powder diffraction (XRD) with a Philips X'Pert Pro Super diffractometer with Cu Kα radiation (λ =1.54178 Å). The field emission scanning electron microscopy (FE-SEM) images were taken on a JEOL JSM-6700F SEM. X-ray photoelectron spectra (XPS) were acquired on an ESCALAB MK II with Mg Kα as the excitation source. The magnetic measurements were carried out with a superconducting quantum interference device magnetometer (Quantum Design MPMS XL-7). The electrical transport property measurements were carried out using a Keithley 4200&SCS Semiconductor Characterization System and a four-point probe method. Differential scanning calorimetry (DSC) was carried out using a NETZSCH DSC 200 F3 machine, in which the sample was sealed in an aluminum pan. The low-temperature in-situ XAFS experimental setup is similar to that in our published paper, which permits the measurement in the range of 5-320 K.[26] In-situ XAFS data at V K-edge at a series of temperatures were recorded in transmission mode at U7B and U7C stations of the National Synchrotron Radiation Laboratory (NSRL), China.

Calculation details. The calculations are performed with the Vienna ab initio simulation package (VASP) code.[27-29] Projector augmented wave (PAW) is used to described the ion-electron interaction.[30] The plane-wave basis set is 400eV cutoff. Exchange and correlation energy is described by Perdew, Burke and Ernzerhof (PBE) functional.[31] The hexagonal super cells consisting of 12 V and 24 S atoms were used in the calculation. The Brillouin zone was sampled by a gamma center grid with 3×3×6 k-point mesh.

Results and discussion

VS_2 sample used in this report was prepared via the solid state reaction as reported previously.[12] Systematical structural characterizations demonstrated the high purity of the as-synthesized sample. As can be seen from the room temperature x-ray diffraction pattern (XRD) of the as synthesized sample (Fig. 1a), all the diffraction peaks could be well indexed to VS_2 (JCPDS, No. 89-1640)[12,32] with no other impurities being detected, demonstrating the high purity of the synthesized VS_2 sample. Meanwhile, it is of note that all the diffraction peaks corresponding to VS_2 were observed from the theta-2theta x-ray diffraction patterns, illustrating that the as synthesized sample is of polycrystalline character, in that if it is one single crystal, only the c-orientation (00l) peaks would be observed in the theta-2 theta x-ray diffraction patterns. And as can be seen from the scanning electron microscopy (SEM) image (Fig. 1b) and the transmission electron microscopy (TEM) image (Supproting Information, Fig. S1), the as synthesized VS_2 with the particle size of about 1μm is indeed of polycrystalline character. Meanwhile, to confirm the high quality of the as synthesized VS2 sample, the X-ray photoelectron spectroscopy (XPS) were also performed. As presented in Fig. S2a and S2b, the binding energy for V $2p_{1/2}$, V $2p_{3/2}$ and S $2p_{3/2}$ are 523.5eV, 516.2eV and 160.6eV, respectively, which were all consistent with the previous reported values,[33] illustrating the high purity of the as-obtained sample. To demonstrate the reversible phase transition characteristics of VS_2 at room temperature, the differential scanning calorimetry (DSC) thermal data of VS_2 was also presented in Fig. S3, from which an obvious endothermic peak at ca. 306.1 K in heating cycle and an exothermic peak at ca. 298.7 K in cooling cycle were clearly observed, indicating the well-defined phase transition. In the meantime, a step-point with a slight increase of thermal conductivity at about 310K as presented in the temperature dependent thermal conductivity measurement (Fig. S4) also demonstrated the room temperature phase transition character.

The thermal anomalies have often been observed across the CDW transition process, which had been reported in TaS_2, $NbSe_2$ et. al.[34] And as can be seen from the DSC curves of the pristine VS_2 (Fig. S3), the evident endothermic peak and exothermic peak further confirm that a distortion of the pristine lattice happened as well along with the variation of electronic properties, demonstrating the strong correlation between the

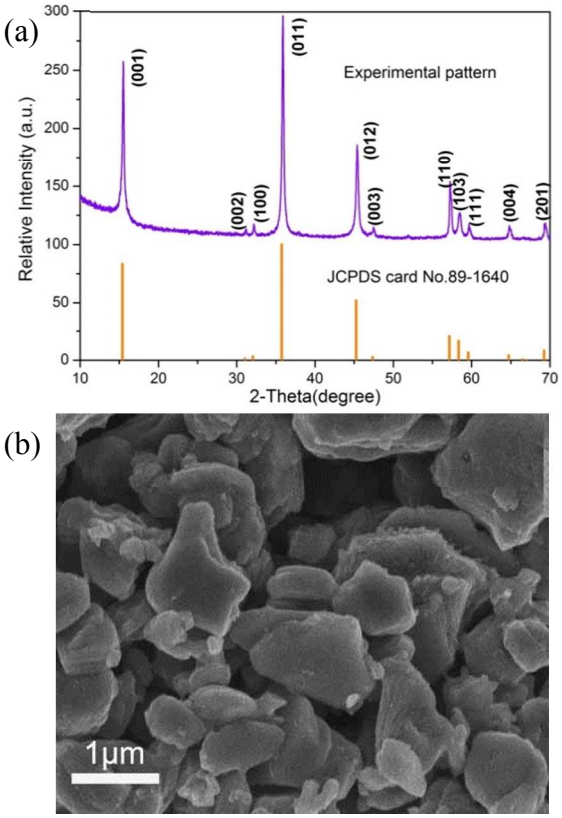

Fig.1 Structure characterization of as-synthesized VS_2. (a) The experimental powder x-ray diffraction pattern and the standard pattern for VS_2 (JCPDS card No. 89-1640), demonstrating the high purity of the as-synthesized sample. (b) Scanning electron microscopy (SEM) image of the synthesized VS_2, from which it can be seen the polycrystalline character of VS_2.

charge carrier density and the lattice deformation, which is in consistence with the CDW behavior as observed in TaS_2, NbS_2 et.al. The more direct evidence for such structural modulations could be identified by temperature-dependent high-resolution transmission electron microscopy (HRTEM) and electron diffraction (ED) measurements (Fig. 2). The HRTEM image of VS_2 at $T>T_{CDW}$ (Fig. 2a) presented well defined hexagonal symmetry, in which the interplanar spacing was measured to be 2.73 Å according to the periodic pattern in the lattice fringe image, matching up with that of the (100) facet of VS_2 (2.784 Å). However, on cooling below the T_{CDW} (Fig. 2b), satellite spots around the initial hexagonal symmetry were clearly observed, which illustrated the appearance of superlattice reflections across CDW transition. And the as-observed superlattice reflections that corresponded to an incommensurate superlattice in real space, demonstrated the appearance of structure variation in the S-V-S plane during the CDW electronic transition process.[23,25] Above the transition temperature, VS_2 belongs to the space group P-3m1, and the V atoms were hexagonally arranged.[32] While, the ED results at $T<T_{CDW}$ distinctly proved a deviation of the atoms from their original positions, which indicated that the V atoms were incommensurately modulated, generating a periodic lattice distortion. All these results elucidated the structure variation during the CDW transition process in pristine VS_2.

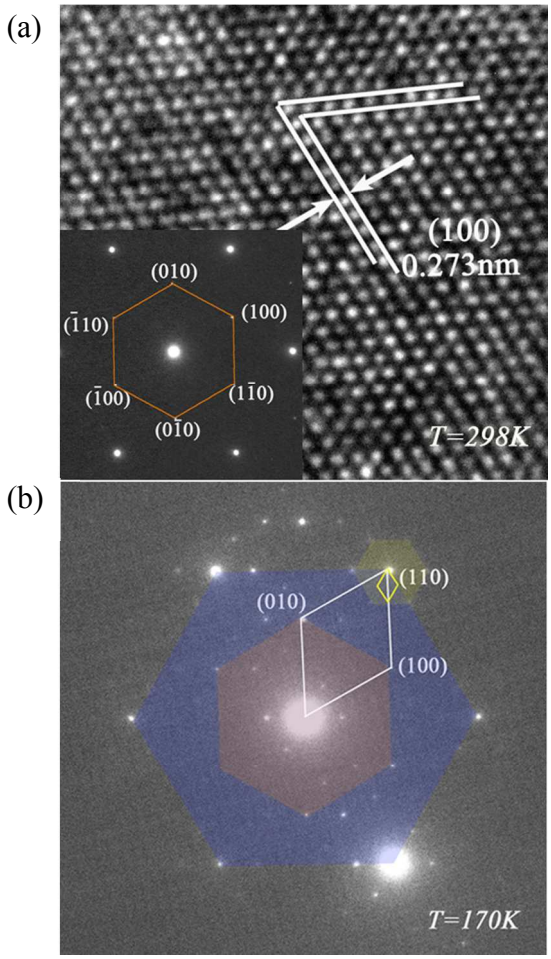

Fig. 2 Structurual characterizations verified across the phase transition in VS_2. (a) HRTEM image of the VS_2 samples at $T>T_{CDW}$. Inset: the corresponding ED patterns. (b) The ED patterns of VS_2 after phase transition at $T< T_{CDW}$.

Meanwhile, the temperature-dependent in-situ XAFS measurement at V K-edge from room temperature to 10 K (Fig. 3) was conducted to further detect these atomic evolutions and to obtain structural information associated with CDW transition. And the details of the fitting process were shown in the supporting information. The single-crystal x-ray diffraction has been reported to be able to detect the superlattice peaks in single crystals.[35] However, the as synthesized VS_2 sample is of the polycrystalline character, thus limiting the application of single-crystal x-ray diffraction. Moreover, the powder x-ray diffraction is unable to detect the CDW superstructure peaks in polycrystalline VS_2, which had already been reported in previous literature.[32] This might be due to the low spatial resolution brought by peak widening of polycrystal in the powder x-ray diffraction patterns. Thus, XAFS, with the advantage of high spatial resolution accuracy (~0.01 Å) to determine the interatomic distances, would be a powerful technique to carry out investigation on the small local structural changes in VS_2 across CDW transition.[26,36] Small variations can be found in the $k\chi(k)$ oscillation shape in the k range of 4–5 $Å^{-1}$ and 9-11 $Å^{-1}$ (Fig. 3a). The Fourier transformed (FT) $k^3\chi(k)$ functions of the V K-edge extended XAFS (EXAFS) as shown in Fig. 3b were characterized by two distinct peaks: the first peak at around 1.8Å was ascribed to the nearest neighbored V–S bond, and the other one at around 2.6 Å was associated to V–V bond. By decreasing temperature, the V–S coordination peak displayed little variations, while the V–V FT peak was intensified and shifted to low k range. In the normal state at high temperature, VS_2 crystallized in the 1T layered structure with CdI_2-type crystalline characteristics, consisting of planes of hexagonally arranged V atoms sandwiched between two S layers (Fig. 3c). And the V–V bond length had an equivalent single value of 3.22 Å, illustrating the equal distance arrangement of vanadium atoms with pristine 1×1 periodicity. In-situ XAFS results implied that, across the CDW transition, partial V_3S tetrahedron configuration composed of three V atoms bonding with one S atom is contracted, that is, V atoms are close to each other while V–S bond length remains constant, forming the V trimers in the local region. The increment of the V–V peak intensity along with the temperature decrement was probably due to the reduced thermal vibration upon cooling process. To our best knowledge, this is the first in situ temperature-dependent XAFS study of the CDW transition of VS_2.

Quantitative structural parameters around V atoms during the CDW transition had also been obtained through a least-squares parameter fitting using the ARTEMIS module of IFEFFIT. It is of note that the as obtained bond length from the Fourier transformed (FT) $k^3\chi(k)$ functions is usually about 0.2-0.5 Å smaller than the actual bong-length obtained via calculation process, due to the scattering phase-shift in sine function of the theoretical expression for EXAFS.[37] And then, the non-linear least squares fitting is adopted to provide the real bond lengths. The V–S and V–V distances among all the best fit parameters were shown in Table 1. And to check the veracity of the fits, we also carried single V-V shell fitting for the data below 280 K, with all the parameters of fits summarized in Table S1 (Supporting Information). It can be seen that there is a significant improvement in the reduced-chi-square, goodness-of-fit and fitting curves by using a split V-V shell for the data below 280 K. For 310 K data, the single-shell fitting strategy has given a good fit result, as can be verified by the small

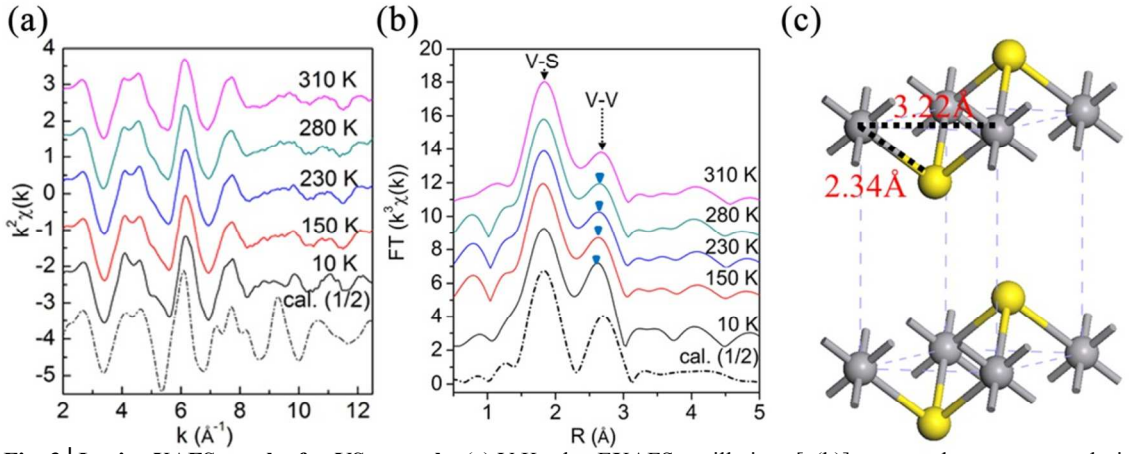

Fig. 3 | In-situ XAFS results for VS_2 sample. (a) V K-edge EXAFS oscillations [χ(k)] at several temperatures during the cooling process. (b) Corresponding Fourier transforms of (a). The dash-dotted line in panel (a) and (b) stands for the calculation result. (c) Atomic structure of hexagonal VS_2 with metal V layer sandwiched between two S layers. Gray and yellow balls denote V and S atoms, respectively.

reduced chi-square and R-factor (goodness-of-fit). This is in consistent with the HRTEM result that VS_2 in normal state is of high symmetry. Hence, we consider that it is unnecessary to perform the two V-V shells fitting for comparison for 310 K data. The fitting results pointed out clearly the bond lengths variations across the CDW process. It could be seen that the V–S bond length of 2.34 Å was almost temperature independent. While, as for the fitted V–V bond, two incoordinate V–V bonds as expected for V trimers formation were obviously observed when the temperature is down to 280 K. The shorter bond length of 3.11 Å is contributed from V–V bond in the vanadium trimers, while the longer one of 3.25 Å is contributed from V–V bond between the trimers. Although the small splitting is less than 5%, the local structural evolution across the CDW

Table I. The structural parameters (distance R, coordination number N and Debye-Waller factor σ^2) for the different V–S and V–V pairs for crystalline VS_2 samples at several temperatures during the cooling process.

Temperature	Bond	R (Å)	N	σ^2 (10^{-3} Å)
310 K	V-S	2.34±0.01	6	3.1±0.3
	V-V	3.22±0.02	6	5.7±0.5
280 K	V-S	2.34±0.02	6	2.9±0.6
	V-V	3.11±0.02	1.9±0.2	5.3±0.5
		3.25±0.01	4.1±0.3	
230 K	V-S	2.34±0.02	6	2.5±0.2
	V-V	3.10±0.02	2.0±0.1	5.1±0.3
		3.26±0.01	4.0±0.3	
150 K	V-S	2.34±0.01	6	2.1±0.2
	V-V	3.09±0.02	2.0±0.1	4.9±0.5
		3.26±0.01	4.0±0.2	
10 K	V-S	2.34±0.02	6	1.9±0.2
	V-V	3.08±0.02	2.0±0.1	4.4±0.5
		3.27±0.01	4.0±0.2	

transition was well demonstrated. In a word, the formation of V trimers with the variation of V-V bonds length along with temperature decrement was well demonstrated.

Temperature dependent measurement of resistivity or magnetization is one of the commonly used methods for the analysis of CDW behaviors. Along with the temperature decrement, "anomalous" behavior in resistivity and magnetic susceptibility can often be observed as reported in the typical CDW material systems, such as 1T-TaS_2, 2H-TaS_2, 2H-NbS_2 and 1T-VSe_2, which provide the direct evidence for the appearance of CDW transition.[10,17,38,39] To study the influence of CDW transition on electronic and magnetic properties of VS_2, the temperature-dependent electrical resistivity and magnetic susceptibility measurements were well performed (Fig. 4), which are the commonly used methods for the analysis of CDW behaviors in transition metal dichalcogenides (TMDs). [10,17,38,39] As can be seen from Fig. 4a, along with the reduction of temperature, a decrease of electrical resistivity was observed, showing the metallic behavior of VS_2. While, a step-point with a slight increase of resistivity appears at around 307 K (amplified in the inset of Fig. 4a), signaling the CDW transition. And below the CDW point, the resistivity continuously decreased, presenting the well-kept metallic character. Fig. 4b showed the temperature dependent magnetization curves for VS_2, from which the CDW transition was also indicated by a step at 307.5 K. It could be clearly seen

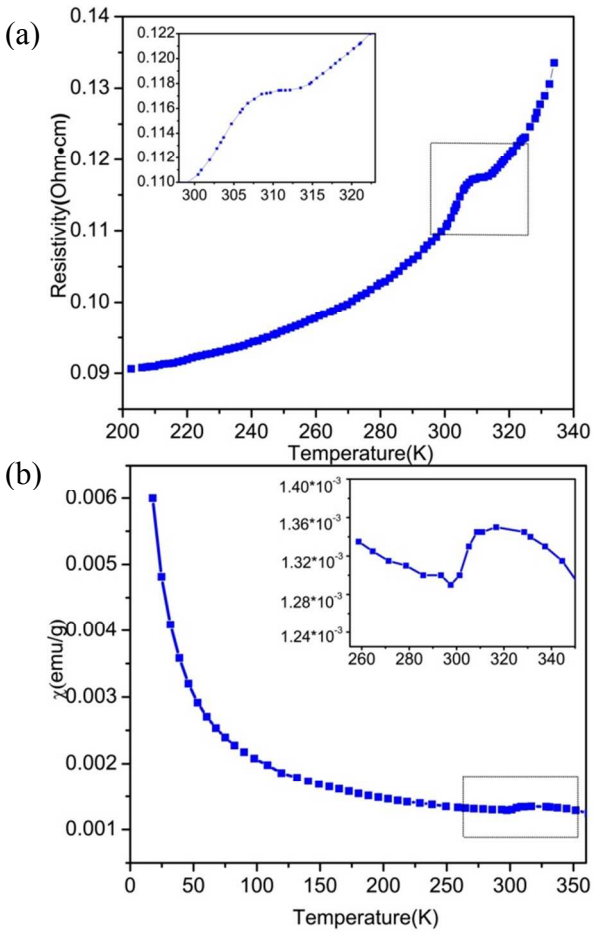

Fig. 4 Temperature dependent electronic and magnetic property measurement. (a) Temperature-dependent electrical resistivity of VS_2. (b) Temperature-dependent magnetization of

that the magnetization decreased to the minimum induced by the structural modulation, and then increased with reducing temperature, which was mainly due to the dominant magnetic contribution of V atoms at low temperature. The above temperature-dependent resistivity presents the intrinsic metallicity of VS_2, while the CDW transition at around 307 K perturbs the electronic structure of VS_2.

To analyze the connection between the observed structure modulation and electronic properties, the corresponding structural models and the theoretical calculations were performed as shown in Fig. 5. For $T > T_{CDW}$, the experimental structure (JCPDS, No. 89-2640), with a fixed V-V bond length of 3.22 Å, was used in DFT calculation. For $T < T_{CDW}$, the system was also modeled based on the high-temperature experimental structure, except that the V-V bond length was fixed to 3.11 and 3.27 Å which correspond to the V-V bonds length inside and between the V trimers, respectively. All those constraints on the V-V bond lengths were kept during the geometry optimization (Fig. 5a and b). Based on our results, though several bands crossed Fermi level, only the a_{1g} band (as shown in Fig. 5c, No.136) was significantly affected by the CDW transition. The local density of states of the a_{1g} band projected above S atoms on one side of VS_2 layer was shown in Supplementary Fig. S5. For the $T > T_{CDW}$ structure (Fig. S5a), there was a 1×1 periodicity for the bright spots, which is the projected charge density of S atoms on the a_{1g} band. For the $T < T_{CDW}$ structure (Fig. S5b), there was a new $\sqrt{3}\times\sqrt{3}$ periodicity for the bright spots (charge density), which reflected directly the variation on charge density as a result of formation of the V trimers. To this point, the formation of V trimers played an important role during the CDW process.

And based on our calculation result, the connections between the observed structure modulation and electronic properties were discussed in detail. As believed, symmetry broken may lead to a reduction on the conductivity, for example, the Peierls transition. In the VS_2 system, for $T < T_{CDW}$, the newly formed $\sqrt{3}\times\sqrt{3}$ periodicity thus will break the pristine symmetry and reduce the conductivity. As well as there were several bands crossed the Fermi level, the formation of V trimers would only lead to a small increase on resistivity rather than a metal-insulator transition when the CDW transition occurred with temperature decreasing, just as what was observed in the experiments (Fig. 4a). Unlike VO_2, where the dimerization and off-axis zigzag displacement of V–V pairs induced a Peierls-like gap at the Fermi level across the metal-insulator transition (MIT), no gap was observed in the CDW transition of VS_2 as shown in the DOS diagram of VS_2 in Fig. 5d, in that the local V trimers only affect the a_{1g} band. Furthermore, the trimerization of V atoms upon the CDW transition also induced a sudden reduction of the magnetization as observed in the inset of Fig. 4b, which was in consistence with previous reports.[25]

As well as observed in other CDW material,[17,38,39] the electrical resistivity of VS_2 still decreased along with the decrement of temperature, exhibiting an obviously metallic character. And in consideration of the always existed V trimers below the transition temperature, it can be concluded that the formed trimers only induced a small saltation on electrical conductivity with the metallic behavior well-kept. Meanwhile, the ground-states density-functional theory (DFT) calculations based on the atomic structural parameters were also performed to demonstrate the remained metallic character. The obtained densities of states (DOS) in Fig. 5d presented the high resides across the Fermi level, revealing the metallic behavior of VS_2 below the phase transition temperature, which was in

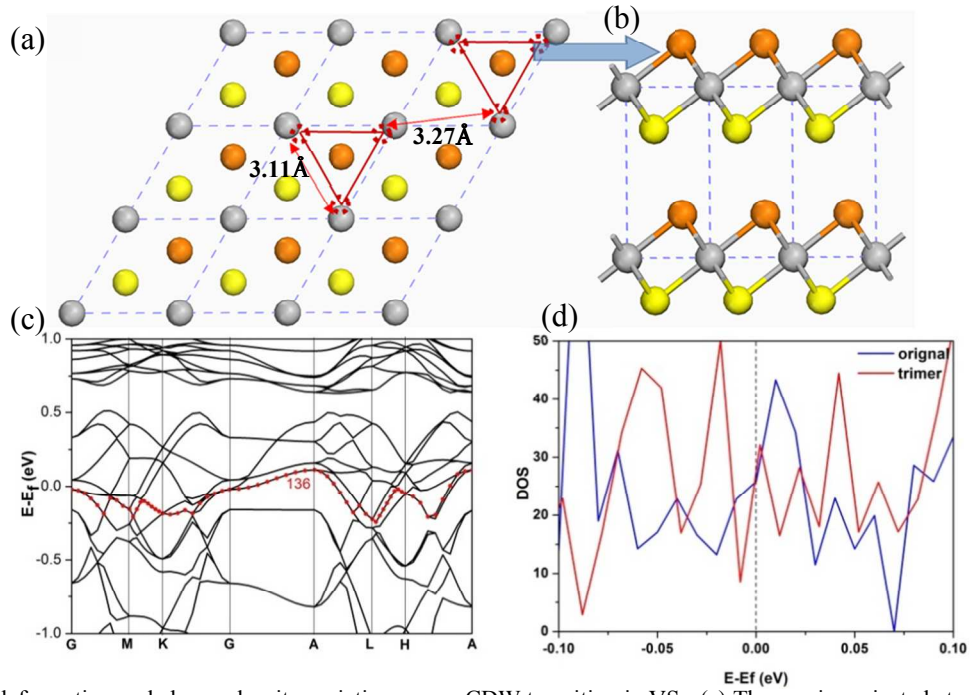

Fig. 5 Lattice deformation and charge-density variation across CDW transition in VS_2. (a) The c-axis projected atomic view of VS_2 and their variations in the CDW ordered phase. The vanadium atoms in the normal state are in gray color, while displacements of the vanadium atoms are marked by red doted circle. The trimerization of vanadium atoms are depicted as red lines. (b) The side-view of VS_2 structure along a-axis direction. (c) The calculated band diagram of VS_2 structure at ground state. (d) DOS diagram of VS_2 before and after phase transition.

consistence with our temperature dependent resistivity measurement result. As it is well known, at a certain temperature range, the phonon scattering plays an important role in electronic conductivity for the metallic material. In consideration of the metallic character of VS_2, the phonon scattering was reduced with the temperature going down due to the decreased lattice order, which was confirmed by the decreased σ^2 of both V–V and V–S pairs shown in Table 1, and finally led to the continuously decreases of electrical resistivity for VS_2. As a consequence, the V trimers formed during the structure modulation process actually influenced the electronic properties of VS_2, while the metallic character was well-kept.

Conclusions

In conclusion, we have unveiled the fine modulation of atomic structure during the CDW transition in VS_2 system via temperature-dependent in-situ XAFS spectroscopy combined with low temperature HRTEM technique. This structural phase transition can be definitely characterized by the formation of local V trimers with the contracted V–V bond length of 3.11 Å, which constantly existed as the temperature decreases apart from T_{CDW}. Meanwhile, it was clearly observed that the electronic properties were also modulated with a saltation on temperature dependent resistivity curves due to the fluctuation of atomic lattice. These results reveal a clear correlation between the dynamics of the lattice structure and electronic properties in VS_2 system, paving the new way for deep analysis of the nature of electronic properties of VS_2 across the CDW transition.

Acknowledgements

This work was financially supported by the National Natural Science Foundation of China (no. 21222101, 11132009, 21331005, J1030412, 11079004, U1232132, 11422547), Chinese Academy of Science (XDB01010300), the Fok Ying-Tong Education Foundation (No. 141042) and the Fundamental Research Funds for the Central Universities (no. WK2060190027, WK2310000024). Zhenpeng Hu at NKU thanks NSFC funding support (No. 21203099) and Doctoral Fund of Ministry of Education of China (20120031120033). The authors are grateful to NSRL for the valuable XAFS beamtime.

Notes and references

[a] Hefei National Laboratory for Physical Sciences at Microscale, University of Science and Technology of China, Hefei 230026, P. R. China, E-mail: czwu@ ustc.edu.cn
[b] National Synchrotron Radiation Laboratory, University of Science and Technology of China, Hefei, 230029, P. R. China, E-mail: sqwei@ ustc.edu.cn
[c] School of Physics, Nankai University, Tianjin, 300071, P. R. China.
†Electronic Supplementary Information (ESI) available. See DOI: 10.1039/b000000x/
† These authors contributed equally to this work.

1 J. Chang, E. Blackburn, A. T. Holmes, N. B. Christensen, J. Larsen, J. Mesot, R. Liang, D. A. Bonn, W. N. Hardy, A. Watenphul, M. v. Zimmermann, E. M. Forgan and S. M. Hayden, *Nat. Phys.* 2012, **8**, 871

2 Y. I. Joe, X. M. Chen, P. Ghaemi, K. D. Finkelstein, G. A. de la Pena, Y. Gan, J. C. T. Lee, S. Yuan, J. Geck, G. J. MacDougall, T. C. Chiang, S. L. Cooper, E. Fradkin and P. Abbamonte, *Nat. Phys.* 2014, **10**, 421..

3 C. D. Malliakas and M. G. Kanatzidis, *J. Am. Chem. Soc.* 2013, **135**, 1719.

4 S. Van Smaalen, *Acta. Cryst.* 2005, **61**, 51.

5 D. Mihailovic, D. Dvorsek, V. V. Kabanov, J. Demsar and S. Trasatti, *Appl. Phys. Lett.* 2002, **80**, 871.

6 N. Ogawa and K.Miyano, Charge-density wave as an electro-optical switch and memory. *Appl. Phys. Lett.* **80**, 3225-3227 (2002).

7 T. L.Adelman, S. V. Zaitsev-Zotov and R. E. Thorne, *Phys. Rev. Lett.* 1995, **74**, 5264.

8 M. Chhowalla, H. S. Shin, G. Eda, L.-J. Li, K. P. Loh and H. Zhang, *Nat. Chem.* 2013, **5**, 263.

9 J. Feng, X. Sun, C. Wu, L. Peng, C. Lin, S. Hu, J. Yang and Y. Xie, *J. Am. Chem. Soc.* 2011, **133**, 17832..

10 K. Xu, P. Chen, X. Li, C. Wu, Y. Guo, J. Zhao, X. Wu and Y. Xie, *Angew. Chem. Int. Ed.* 2013, **52**, 10477..

11 C. Lin, X. Zhu, J. Feng, C. Wu, S. Hu, J. Peng, Y. Guo, L. Peng, J. Zhao, J. Huang, J. Yang and Y. Xie, *J. Am. Chem. Soc.* 2013, **135**, 5144.

12 J. Feng, L. Peng, C. Wu, X. Sun, S. Hu, C. Lin, J. Dai, J. Yang and Y. Xie, *Adv. Mater.* 2012, **24**, 1969.

13 X. Sun, J. Dai, Y. Guo, C. Wu, F. Hu, J. Zhao, X. Zeng and Y. Xie, *Nanoscale* 2014, **6**, 8359..

14 RadisavljevicB, RadenovicA, BrivioJ, GiacomettiV, KisA, *Nat. Nano*. 2011, **6**, 147.

15 Q. H. Wang, K. Kalantar-Zadeh, A. Kis, J. N. Coleman, M. S. Strano, *Nat. Nano.* 2012, **7**, 699.

16 RadisavljevicB, RadenovicA, BrivioJ, GiacomettiV and KisA, *Nat. Nano* 2011, **6,** 147

17 J. A. Wilson, F. J. Di Salvo and S. Mahajan, *Phy. Rev. Lett.* 1974, **32**, 882.

18 A. H. Castro Neto, *Phy. Rev. Lett.* 2001, **86**, 4382.

19 D. W. Shen, B. P. Xie, J. F. Zhao, L. X. Yang, L. Fang, J. Shi, R. H. He, D. H. Lu, H. H. Wen and D. L. Feng, *Phy. Rev. Lett.* 2007, **99**, 216404.

20 P. Goli, J. Khan, D. Wickramaratne, R. K. Lake and A. A. Balandin, *Nano Lett.* 2012, **12**, 5941. .

21 P. Hajiyev, C. Cong, C. Qiu and T. Yu, *Sci. Rep*. 2013, **3**, 2593.

22 L.-Y. Gan, Q.Zhang, Y. Cheng and U. Schwingenschlögl, *Phys. Rev. B2013,* **88**, 235310.

23 N. Katayama, M. Uchida, D. Hashizume, S. Niitaka, J. Matsuno, D. Matsumura, Y. Nishihata, J. Mizuki, N. Takeshita, A. Gauzzi, M. Nohara and H. Takagi, *Phy. Rev. Lett.* 2009, 103, 146405..

24 T. Tsuda, H. Yasuoka and Y. KitaokaJ, *Mag. Mag. Mater.* 1983, **31**, 1101.

25 M. Mulazzi, A. Chainani, N. Katayama, R. Eguchi, M. Matsunami, H. Ohashi, Y. Senba, M. Nohara, M. Uchida, H. Takagi, S. Shin, *Phy. Rev. B* 2010, **82**, 075130.

26 T. Yao, X. Zhang, Z. Sun, S. Liu, Y. Huang, Y. Xie, C. Wu, X. Yuan, W. Zhang, Z. Wu, G. Pan, F. Hu, L. Wu, Q. Liu, S. Wei, *Phy. Rev. Lett.* 2010, **105**, 226405.

27 G. Kresse and J. Furthmüller, *Comput. Mater. Sci.* 1996, **6**, 15.

28 G. Kresse and J. Hafner, *Phys. Rev. B* 1993, **47**, 558.

29 G. Kresse and J. Furthmüller, *Phys. Rev. B* 1996, **54**, 11169.

30 P. E. Blöchl, *Phys. Rev. B* 1994, **50**, 17953

31 J. P.Perdew, K. Burke and M. Ernzerhof, *Phys. Rev. Lett.* **1996**, 77, 3865

32 D. W. Murphy, C. Cros, F. J. Di Salvo and J. V. Waszczak, *Inorg. Chem.* 1977, **16**, 3029.

33 C. S. Rout, B.-H. Kim, X. Xu, J. Yang, H. Y. Jeong, D. Odkhuu, N. Park, J. Cho, H. S. Shin, *J. Am. Chem. Soc.* 2013, **135**, 8720.

34 J. M. E. Harper, T. H. Geballe and F. J. Di Salvo, *Phys. Rev. B* 1977, **15**, 2943.

35 C. D. Malliakas and M. G. Kanatzidis, *J. Am. Chem. Soc.* 2013, **135**, 1719.

36 X. G. Tan, T. Yao, R. Long, Z. H. Sun, Y. J. Feng, H. Cheng, X. Yuan, W. Q. Zhang, Q. H Liu, C. Z. Wu, Y. Xie and S. Q. Wei, *Sci. Rep.* 2012, **2**, 466.

37 E. A. Stern, D. E. Sayers and F. W. Lytle, *Phys. Rev. B* 1975, **11**, 4836.

38 H.Mutka, L. Zuppiroli, P. Molinié and J. C. Bourgoin, *Phys. Rev. B* 1981, **23**, 5030.

39 A. H. Thompson and B. G. Silbernage, *Phys. Rev. B* 1979*,* **19**, 3420.